Supplemental Information

The T-cell receptor is a structure capable of initiating signalling in the absence of large conformational rearrangements

Ricardo A. Fernandes, David A. Shore, Mai T. Vuong, Chao Yu, Xueyong Zhu,

Selma P. Periera-Lopes, Heather Brouwer, Janet A. Fennelly, Charlotte Whicher, William Gao,

Claire M. Jessup, Edward J. Evans, Ian A. Wilson, Simon J. Davis

Supplemental Figures

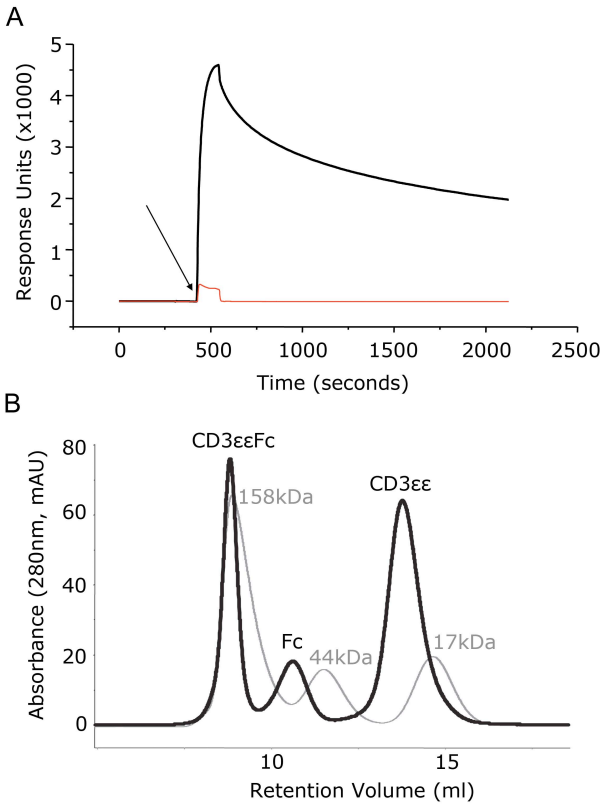

Figure S1. Formation of a stable homodimer of soluble mCD3ε ectodomains, related to Figure 1 and 2. A. mCD3εε binds the conformation-sensitive mAb 17A2, as determined in a surface plasmon resonance-based assay as implemented by Biacore™. Approximately 5,000 response units of an antibody specific for mouse IgG Fc was immobilised on the surface of a CM5 Biacore™ chip using standard amine coupling. mCD3ααFc (black trace) or an equivalent amount of a control IgG-Fc protein (red trace) was then injected and captured at the surface of separate flow cells. Following washing, the conformation-specific mAb 17A2 was injected over both flow cells, at a protein concentration of 0.01 mg/ml (arrow). **B.** Size exclusion gel filtration of the purified mCD3εε. A mixture of mCD3εεFc, IgG Fc and mCD3εε, respectively (black trace), resulting from the "on-column" thrombin digestion of protein A-immobilized mCD3εεFc, was separated using a Hi-load Superdex 75 column. Approximately 100µg of total protein was loaded. The peak fraction is estimated to contain mCD3εε at a concentration of ~2.5 µM. The profile of molecular weight markers is overlaid for reference (grey trace). Free CD3ε monomer was undetectable suggesting that the homodimer is stable at submicromolar concentrations.

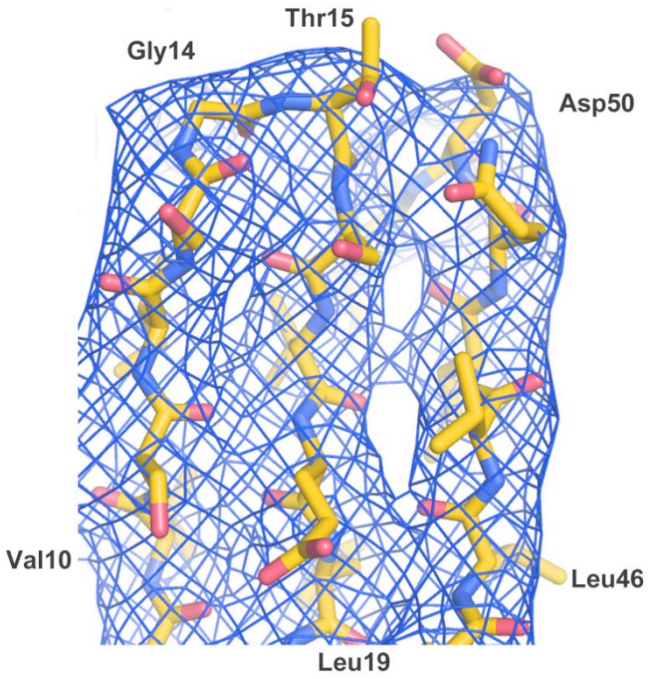

Figure S2. $2F_o$-F_c electron density for the final refined model of mCD3ε, related to Figure 1. Representative electron density is shown for Leu46-Asp50 and Val10-Leu19 of mCD3ε in complex with the 2C11 Fab (complex A) in a σ_A-weighted 2Fo-Fc map contoured at 1.0 σ.

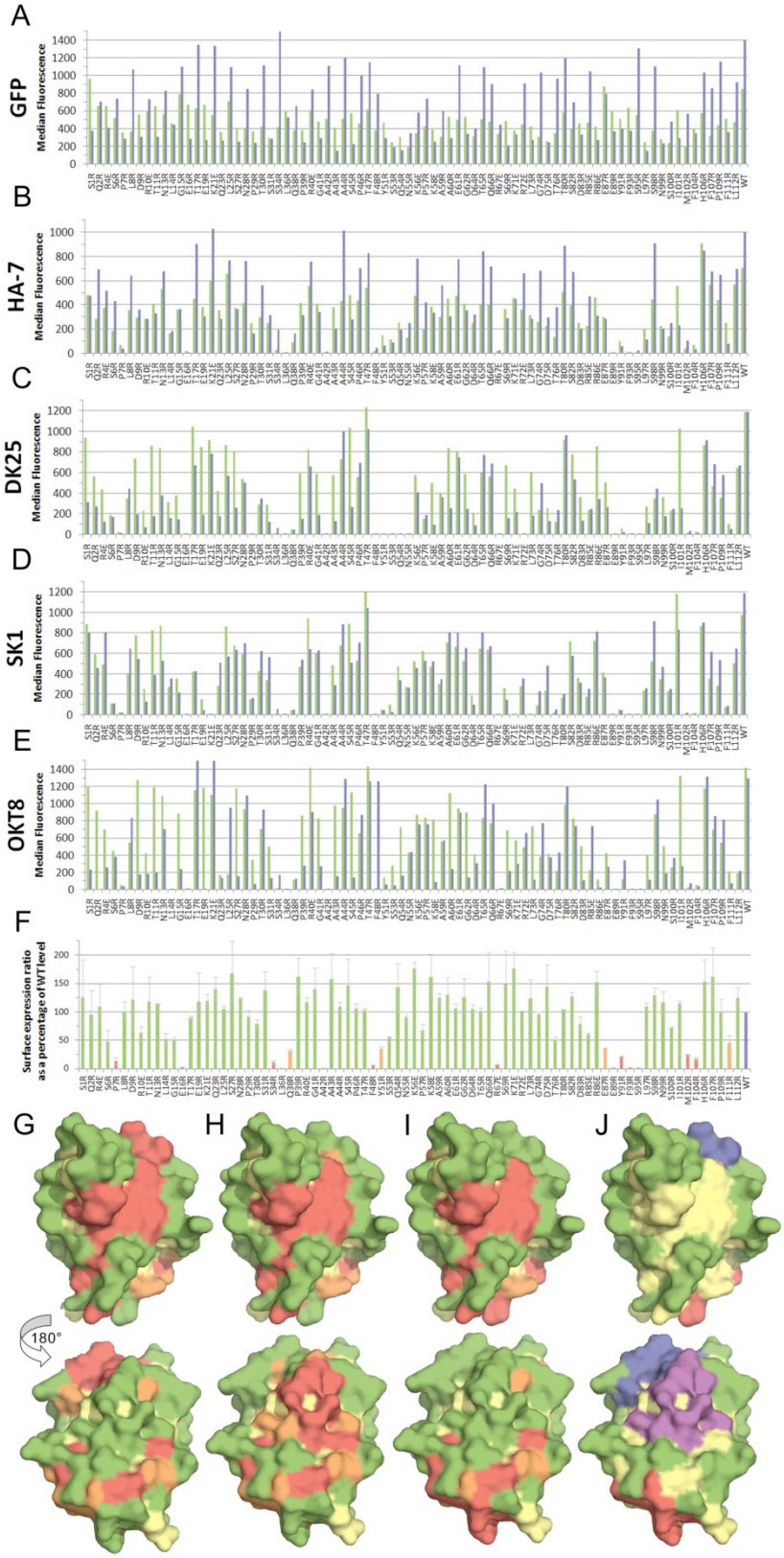
A
GFP
Median Fluorescence
B
HA-7
Median Fluorescence
C
DK25
Median Fluorescence
D
SK1
Median Fluorescence
E
OKT8
Median Fluorescence
F
Surface expression ratio as a percentage of WT level
G
H
I
J
180°

Figure S3. Cell surface expression and antibody staining of mutant forms of hCD8α, related to Figure 4. A. GFP expression in Jurkat cells transduced in duplicate (green, blue bars) with lentiviral vectors encoding HA-tagged CD8α mutants and, following an IRES sequence, GFP (as an indicator of the efficiency of viral transduction). **B-E.** Median fluorescence for FACS analysis of the cells using monoclonal antibodies specific for the HA tag (HA-7, **B**) or CD8α (mAb DK25, **C**; mAb SK1, **D**; mAb OKT8, **E**). **F**. Histogram showing normalized surface expression levels of the mutated HA-tagged CD8 proteins. The surface expression ratio was calculated as the median fluorescence of anti-HA antibody binding divided by the median fluorescence of IRES-encoded GFP, each determined by FACS. This was normalised against the value obtained for the wild-type protein in the same experiment and the average value for at least two experiments, expressed as a percentage, is shown along with standard errors of the mean. This histogram is the same as that in Fig. 4A, shown for comparison. **G-I**. The surface of CD8α (taken from pdb 1AKJ; Gao et al., 1997) is shown in yellow and individual residues are coloured according to whether their drastic mutation affects binding of monoclonal antibodies DK25 (**G**), SK1 (**H**) or OKT8 (**I**). Residues are coloured as in Fig. 4B. In each panel, the upper view is of the GFCC'C" face and the lower view has been rotated 180° about the vertical axis. **J**. Residues whose drastic mutation affects cell surface expression are coloured yellow, and those whose mutation has no effect on antibody binding are coloured green. The remaining residues are coloured blue, purple and red if their drastic mutation drastically reduces (>85%) the binding of the anti-CD8 mAbs DK25, SK1 or OKT8, respectively, or the mutation mildly affects antibody binding (by 60-85%) and the residue is adjacent to another whose mutation does have drastic effects. This slightly expands the epitopes mapped in Fig. 4D.

Figure S4. Cell surface expression of mutant forms of CD3ε, related to Figure 5. A Histogram showing comparable GFP expression in Jluc^{hi} cells transduced with vectors encoding HA-tagged CD3ε mutants and, from an IRES sequence, GFP. **B.** Histogram showing the HA staining of Jluc^{hi} cells expressing each HA-tagged CD3ε mutant. Bars are coloured as in Fig. 4A. **C**. Histogram of the normalised cell surface expression levels of each CD3ε mutant, calculated by comparing the ratio of median HA staining to median GFP fluorescence for each mutant with that of the wild-type protein, expressed as a percentage. The data shown are representative of two separate experiments; means of triplicates and standard deviations are shown.

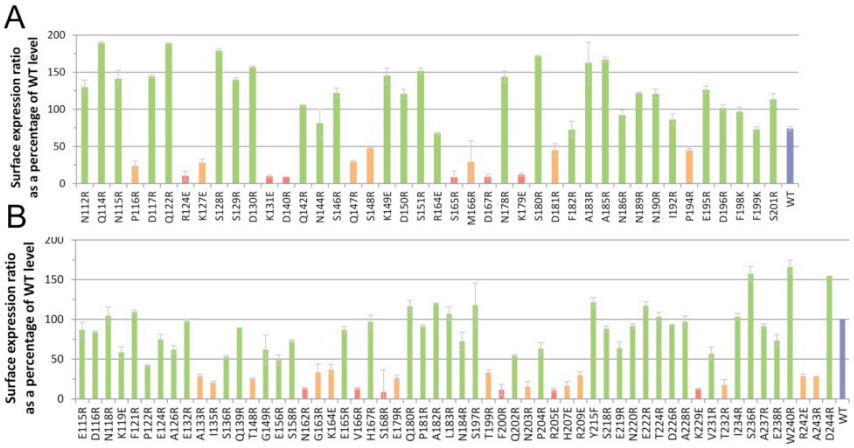

Figure S5. Cell surface expression of mutant forms of TCRα and β, related to Figure 6. Histograms showing the normalised cell surface expression levels of the HA-tagged TCRα (**A**) and TCRβ (**B**) mutants, calculated by comparing the ratio of median HA staining to median GFP fluorescence for each mutant with that of the wild-type protein, expressed as a percentage. Bars are coloured as in Fig. 4A.

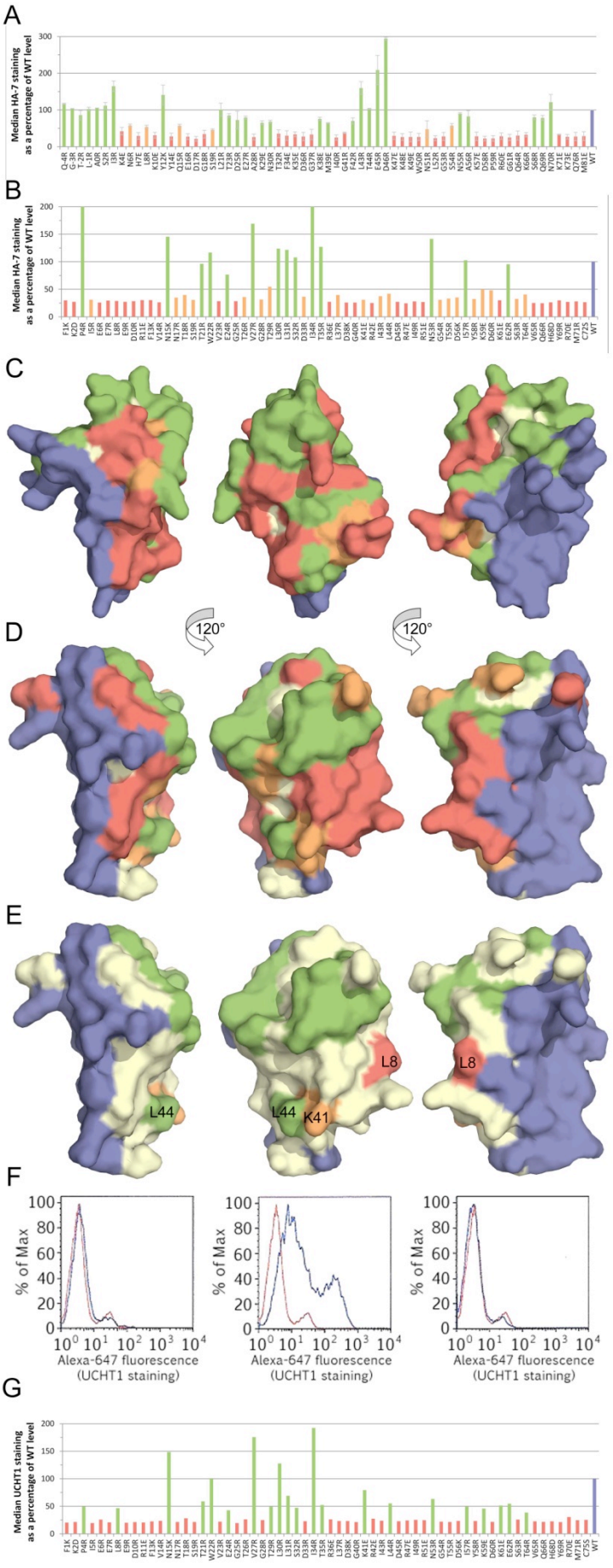
A
Median HA-7 staining as a percentage of WT level
B
Median HA-7 staining as a percentage of WT level
C
D
120°
120°
E
L44
L8
L44
K41
L8
F
% of Max
Alexa-647 fluorescence (UCHT1 staining)
% of Max
Alexa-647 fluorescence (UCHT1 staining)
% of Max
Alexa-647 fluorescence (UCHT1 staining)
G
Median UCHT1 staining as a percentage of WT level

Figure S6. Cell surface expression of mutant forms of CD3γ and δ, related to Figure 6. Histograms showing the normalised cell surface expression levels of the HA-tagged CD3γ (**A**) and CD3δ (**B**) mutants. The weak expression of the HA-tagged proteins meant that only the most highly infected cells (GFP fluorescence > 100) could be analysed, and that the expression levels could not be normalized against GFP levels. The ratios of median anti-HA antibody staining for the mutant and wild-type proteins, expressed as percentages, are shown. Bars are coloured according to whether the mutations had large effects (red: median HA staining <44% of WT for CD3γ, <30.5% for CD3δ); weaker effects (orange: median HA staining 44-60% of WT for CD3γ, 30.5-60% for CD3δ); or no substantial effects (green). **C-E.** Three views of the surface of CD3γ (**C**; from pdb 1SY6; (1)) and of CD3δ (**D, E**; from pdb 1XIW; (2)), related by 120° rotations about the vertical axis. In **C** and **D**, residues coloured blue are buried in interactions with CD3ε (1,2). Mutated residues are coloured as in A, B according to the effects of the mutations. In **E**, residues are coloured as in D, except that residues whose drastic mutation prevented CD3δ from facilitating the expression of CD3ε at the surface of 293T cells, presumably due to folding effects, are coloured yellow. **F.** FACS analysis of 293T cells transfected with CD3ε alone (left), CD3ε and CD3δ (middle) or CD3ε and CD3γ (right) stained with the anti-CD3ε mAb UCHT1. Correctly folded CD3δ, but not CD3γ, is sufficient for surface expression of the heterodimer in these cells (in contrast to Jurkat T-cells, see Fig. 5A). **G**. Median fluorescence following UCHT1 staining of 293T cells transfected with WT CD3ε and each mutant of CD3δ, normalised against the level of CD3ε expression obtained inco-transfections with WT CD3δ.

Supplemental Tables

Table S1. Data collection and refinement statistics for the crystal structures of 2C11 Fab and mCD3ε/2C11 Fab complex, related to Figure 1.

Table 1. Data collection and refinement statistics.

Data set	2C11 Fab	mCD3 εε /2C11 Fab
Space group	$P2_1$	$I4_132$
Unit cell (Å)	a = 106.2 b = 72.4 c = 127.5	$a = b = c$ = 263.2
Unit cell (deg.)	$\alpha = \gamma = 90$ β= 109.5	$\alpha = \beta = \gamma = 90$
Resolution (Å) [a]	40.0-2.5 (2.59-2.50)	50.0-4.10 (4.25-4.10)
X-ray source	APS 23-ID	APS 23-ID
Unique reflections	62,077	12,153
Redundancy [a]	3.5 (2.8)	4.3 (4.0)
Average I/σ(I) [a]	8.1 (1.5)	9.7 (2.3)
Completeness [a]	98.6 (90.6)	96.9 (98.4)
R_{sym} [b, a]	0.16 (0.60)	0.09 (0.55)
Molecules in a.u.	4	1
V_m (Å^3/Da)	2.5	6.8
Reflections used in refinement	62,054	12,110
Refined residues	1716	511
Refined waters	409	-
R_{cryst} [c]	0.19	0.22
R_{free} [d]	0.24	0.28
B-values (Å^2)		
Protein	60.8	180.7 [e]
Waters	50.9	-
Ramachandran plot (%)	90.8, 8.8, 0.1, 0.3	75.6, 22.0, 1.6, 0.9
rmsd bond (Å)	0.010	0.010
rmsd angle (deg.)	1.2	1.4

[a] Parenthesis denote outer-shell statistics.

[b] $R_{sym} = \sum_h\sum_i|I_i(h) - \langle I(h)\rangle| / \sum_h\sum_i I_i(h)$, where $\langle I(h)\rangle$ is the average intensity of i symmetry-related observations of reflections with Bragg index h.

[c] $R_{cryst} = \sum_{hkl}|F_o - F_c| / \sum_{hkl}|F_o|$, where F_o and F_c are the observed and calculated structure factors.

[d] R_{free} was calculated as for R_{cryst}, but on 5% of data excluded before refinement.

[e] The B-value is somewhat meaningless at this resolution

Supplemental Experimental Procedures

Expression of a stable CD3ε homodimer

Constructs encoding the mature mouse CD3 ectodomain fragments, preceded by the leader sequence from mouse CD4, were amplified by from T cell cDNA, and cloned into a vector containing the Fc region of mouse IgG1 followed by a hexahistidine motif at the carboxyl-terminus. Cysteines within the conserved *Cys-X-X-Cys-X-Glu* motif of all three CD3 subunits, as well as positions 220, 223 and 225 of the murine Fc region were mutated to serine to preclude aberrant disulphide bonding during protein expression. A thrombin protease recognition sequence (LVPRGS) was introduced at the CD3/Fc interface by mutations Ile213Leu, Asp217Gly and Cys218Ser in mouse Fc. The amplified gene was sub-cloned into the pEFBos expression vector (3) using Nhe1 and Xba1 restriction endonucleases. These vectors were co-transfected into Chinese hamster ovary (CHO) cells together with the glutamine synthetase-encoding expression vector pEE14 (4), using the Fugene lipid transfection reagent (Roche). Clones recombinant for the pEE14 plasmid were selected in media containing 15 μM methionine sulfoxamine and those expressing mCD3Fc were identified by Western blot using antibodies specific for mouse Fc. Despite poor expression of the CD3δ and CD3γ ectodomains in this system, clones expressed high levels of CD3εFc (1-3 mg/L). Cells were grown in DMEM supplemented with 5mM Na Butyrate, 2% L-glutamine, 1% Pen/Strep/Neo antibiotic solution and 10 % ultra-low IgG FCS (Invitrogen). mCD3εFc protein was isolated from concentrated tissue culture supernatant by metal affinity chromatography using Ni-NTA beaded agarose (Qiagen). Soluble mCD3ε ectodomain was isolated by cleavage with bovine thrombin protease (Calbiochem; 3U/mg) for 3 hours at 37°C and purified to homogeneity by size exclusion gel filtration chromatography using a AKTA FPLC fitted with a HiLoad Superdex 75 10/30 column (GE Healthcare) in HBS (25 mM HEPES pH 7.5, 150mM NaCl, 0.04% NaN_3). mCD3ε eluted from the column with a hydrodynamic volume of approx. 15 ml, between the 44 kDa and 17 kDa molecular weight markers, indicating mCD3ε was present in solution as a non-covalent mCD3εε homodimer (**Fig. S1b, Supplemental Information**). The absence of monomeric CD3ε throughout the purification process suggests that homodimerisation is requisite for its stability in solution.

Preparation of 2C11 Fab and purification of the mCD3εε/2C11 Fab complex

The 145-2C11 hybridoma was obtained from Dr Andrew Bushell of the Nuffield Department of Surgery, University of Oxford. Cells were cultured in RPMI (Sigma-Aldrich) and the monoclonal antibody purified from concentrated, cell-free tissue culture supernatant by affinity chromatography using agarose-coupled protein A (Sigma-Aldrich). The 2C11 Fab was isolated by digestion with papaya papain protease, (10 ng/mg) for 4 hours at 37°C, and purified by affinity chromatography using agarose-beaded protein A to remove the Fc region (Sigma-Aldrich). The amino-acid sequence of the 2C11 Fab was determined by sequencing cDNA produced by RT-PCR from mRNA extracted from the 2C11 hybridoma cells. The mCD3εε/2C11 complex was formed by addition of mCD3εε to 2C11 Fab at a molar ratio of

1:2 i.e. with the Fab in excess. The 2C11 Fab bound mCD3εε with nanomolar affinity and the complex was purified by size exclusion chromatography on a HiLoad Superdex 200 10/30 column (GE Healthcare) in HBS.

Structural determination, refinement and validation of the 2C11 Fab and mCD3εε/2C11 complex

The 2C11 and mCD3εε/2C11 structures were determined by molecular replacement, using the program Phaser (5). Mouse mAb IgG2a CNJ206 Fab (pdb 1kno; (6)) and a model built from the human CD3ε (pdb 1sy6; (1)) were the search models for the 2C11 Fab and mouse CD3ε, respectively. Model building was carried out using the programs O (7) and Coot (8), and Refinement was carried out using REFMAC5 (9) and Buster (10). For the refinement of 2C11, non-crystallographic symmetry (NCS) restraints were applied during the initial stages of refinement, but released in the final refinement stage. Due to high solvent content, the refinement of the moderate resolution (4.1 Å) structure of mCD3εε/2C11 was completed with good statistics (**Supplemental Table 1**), and the final model fit the electron density very well (**Fig. S2, Supplemental Information**). The final coordinates were validated using the Joint Center for Structural Genomics (JCSG) quality control server (v2.3), which includes MolProbity (11). Atomic coordinates and structure factors for 2C11 Fab and mCD3ε/2C11 Fab complex have been deposited in the Protein Data Bank with accession numbers 3R06 and 3R08, respectively.

Identification of residues for mutation

In order to identify residues whose side chains were surface exposed and, therefore, suitable for mutation, CD8α, individual CD3 chains or the TCRαβ heterodimer were analysed using the program NACCESS (12). Residues were considered for mutation if any atom had an exposed surface area >5Å^2 (CD3ε) or if 50% or more of their side-chain atoms had an atomic accessibility of >5Å^2 (all other subunits). Residues for which the side chain was clearly involved in hydrophobic interactions within the IgSF domain were excluded even if they fulfilled these criteria. In addition, glycine residues were examined manually in the crystal structures and were mutated if the Cα atom was positioned so that an outward pointing, solvent-exposed side chain could be added without inducing clashes with other residues. In some cases, further residues were excluded from analysis (*e.g.* those already known to be involved in an interaction) as described in the text.

Choice of drastic mutations

The aim of these mutations was to disrupt any interaction that buries the residue being mutated. Therefore, mutations that increase (rather than remove or decrease) side-chain bulk were desirable. The introduction or reversal of charge would also be disruptive. Addition of hydrophobic side chains, however, was not deemed desirable as this may decrease the solubility of recombinant protein and lead to increased aggregation or non-specific

association. The bulkiest charged side chain available is that of arginine, so all residues were mutated to arginine except those that were already positively charged (Arg, Lys, His), which were mutated to glutamic acid.

Constructs

A cassette encoding a standard signal peptide (derived from human RPTP) followed by an HA tag (as defined by Sigma) was cloned into a lentiviral expression vector based on pHR-SIN (13) already encoding an IRES sequence and GFP downstream of the insertion site, *via* BglII (5') and BamHI (3'). This vector allows for the expression of GFP in addition to the desired construct to act as a control for transfection efficiency. hCD8α, hTCR and hCD3 genes were amplified from plasmid templates and cloned into this vector using the BamHI and XhoI restriction sites (using compatible enzymes where necessary). Constructs started from the codon encoding the first amino acid of the mature protein and continued through the stop codon. Mutations were introduced by PCR and final constructs were checked by dideoxy sequencing.

Flow cytometry and analysis

Samples were stained on ice in the dark in PBS, 0.05% sodium azide using monoclonal antibodies specific for HA (HA-7, Sigma, Gillingham, UK) and hTCRαβ (Caltag, Burlingame, CA; directly conjugated to R-Phycoerythrin) for 30 mins. After washing, they were then stained with zenon anti-mouse IgG1 Alexa 647 (Invitrogen, Paisley, UK) for 30 mins. Cells were fixed in 2%, PFA 0.05% sodium azide in PBS for 30 mins. 10,000 live cells were collected on a CyAn FACS machine (Dakocytomation, Glostrup, Denmark) and the data was analysed using FlowJo software version 8.7.3 (Treestar, Ashland, OR). After compensation for overlap between fluorescence channels, live, hTCRαβ positive populations were selected. Pseudo-colour dot plots of GFP expression versus HA-7 staining of these cells were produced and their median fluorescence in each channel was used for data analysis as described in the main text.

Lentiviral transduction of cell lines

293T cells were transiently transfected with pHR-SIN vector constructs, together with pMD.G and p8.91 lentiviral vectors (14) in 6-well plates using Genejuice (Merck, Darmstadt, Germany) according to the manufacturer's instructions. Supernatant was harvested at 48-72hrs after transfection and centrifuged at 2000rpm for 5mins at RT to remove cell debris. $1x10^6$ cells in 0.5ml JMEM (10% FCS 2% L-glutamine, 1% Pen/Strep/Neo, 1% Hepes and 1% Sodium Pyruvate in RPMI 1640) were transduced using this supernatant overnight.

Supplemental References

1. Kjer-Nielsen, L., Dunstone, M. A., Kostenko, L., Ely, L. K., Beddoe, T., Mifsud, N. A., Purcell, A. W., Brooks, A. G., McCluskey, J., and Rossjohn, J. (2004) *Proc. Natl. Acad. Sci. U. S. A.* **101**, 7675-7680

2. Arnett, K. L., Harrison, S. C., and Wiley, D. C. (2004) *Proc. Natl. Acad. Sci. U. S. A.* **101**, 16268-16273

3. Mizushima, S., and Nagata, S. (1990). *Nucleic Acids Res.* **18**, 5322

4. Bebbington, C.R., Renner, G., Thomson, S., King, D., Abrams, D., and Yarranton, G.T. (1992). *Biotechnology. (N. Y).* **10**, 169-175

5. McCoy, A.J. (2007). *Acta Crystallogr. D. Biol. Crystallogr.* **63**, 32-41

6. Charbonnier, J.B., Carpenter, E., Gigant, B., Golinelli-Pimpaneau, B., Eshhar, Z., Green, B.S., and Knossow, M. (1995). *Proc. Natl. Acad. Sci. USA* **92**, 11721-11725

7. Jones, T.A., Zou, J.Y., Cowan, S.W., and Kjeldgaard, M. (1991). *Acta Crystallogr. A.* **47**, 110-119

8. Emsley, P., and Cowtan, K. (2004). *Acta Crystallogr. D. Biol. Crystallogr.* **60**, 2126-2132

9. Murshudov, G.N., Vagin, A.A., and Dodson, E.J. (1997). *Acta Crystallogr. D. Biol. Crystallogr.* **53**, 240-255

10. Blanc, E., Roversi, P., Vonrhein, C., Flensburg, C., Lea, S.M., and Bricogne, G. (2004). *Acta Crystallogr. D. Biol. Crystallogr.* **60**, 2210-2221

11. Richardson, J.S., Bryan, W.A., 3rd, and Richardson, D.C. (2003). *Methods Enzymol.* **374**, 385-412

12. Hubbard, S.J., and Thornton, J.M. (1993). naccess. Department of Biochemistry and Molecular Biology, University College London

13. Bainbridge, J.W., Stephens, C., Parsley, K., Demaison, C., Halfyard, A., Thrasher, A.J., and Ali, R.R. (2001). *Gene Ther.* **8**, 1665-1668

14. Naldini, L., Blomer, U., Gallay, P., Ory, D., Mulligan, R., Gage, F.H., Verma, I.M., and Trono, D. (1996). *Science* **272**, 263-267